AGU PUBLICATIONS

Geophysical Research Letters

Radiocarbon Content of Dissolved Organic Carbon in the South Indian Ocean

S. K. Bercovici[1,2] (iD), A. P. McNichol[3], L. Xu[3] (iD), and D. A. Hansell[1] (iD)

[1]Department of Ocean Sciences, University of Miami, Key Biscayne, FL, USA, [2]Polar Science Center, University of Washington, Seattle, WA, USA, [3]Department of Geology and Geophysics, Woods Hole Oceanographic Institution, Woods Hole, MA, USA

Abstract We report four profiles of the radiocarbon content of dissolved organic carbon (DOC) spanning the South Indian Ocean (SIO), ranging from the Polar Front (56°S) to the subtropics (29°S). Surface waters held mean DOC $\Delta^{14}C$ values of -426 ± 6‰ (~4,400 ^{14}C years) at the Polar Front and DOC $\Delta^{14}C$ values of -252 ± 22‰ (~2,000 ^{14}C years) in the subtropics. At depth, Circumpolar Deep Waters held DOC $\Delta^{14}C$ values of -491 ± 13‰ (~5,400 years), while values in Indian Deep Water were more depleted, holding DOC $\Delta^{14}C$ values of -503 ± 8‰ (~5,600 ^{14}C years). High-salinity North Atlantic Deep Water intruding into the deep SIO had a distinctly less depleted DOC $\Delta^{14}C$ value of -481 ± 8‰ (~5,100 ^{14}C years). We use multiple linear regression to assess the dynamics of DOC $\Delta^{14}C$ values in the deep Indian Ocean, finding that their distribution is characteristic of water masses in that region.

1. Introduction

The global ocean contains a massive reservoir of dissolved organic carbon (DOC), rivaling the atmosphere's pool of CO_2 (Hansell et al., 2009). Greater than 95% of this carbon is stored in the deep ocean, where the dynamics of its cycling remain poorly understood. The radiocarbon signatures for DOC provide information on its lifetime and are thus crucial for understanding the pool's dynamics. Previously published ^{14}C data indicate that ^{14}C ages of DOC at depth range from ~4,000 in the North Atlantic to ~6,500 ^{14}C years in the North Pacific (Druffel et al., 1992; Druffel & Griffin, 2015), suggesting some DOC fractions persist in the ocean's deep layers for millennia. However, this age range is indicated from relatively few water column profiles in the global ocean. Radiocarbon profiles have not previously been reported for the Indian Ocean, an important system in considering meridional overturning circulation, as its deep waters comprise ~35% of the source waters to the circumpolar waters in the Southern Ocean (SO), the origin of abyssal waters in all major ocean basins (Schmitz, 1995; Talley, 2013). Here we present four ^{14}C profiles of DOC (DOC $\Delta^{14}C$) in the South Indian Ocean (SIO), finding that DOC $\Delta^{14}C$ values there are distinguishable by water mass.

1.1. Hydrography of the Indian Ocean

The Indian Ocean is zonally confined by Africa in the west, and Asia and Australia in the east. The Agulhas Current (the western boundary current of the SIO) flows poleward, opposite to the northward Circumpolar Deep Waters and Antarctic Bottom Waters (both of these waters are hereafter generalized as CDW) (Beal et al., 2006; Gordon, 1985; Schmitz, 1995). North Atlantic Deep Water (NADW; identified by its high salinity core) exits the Atlantic south of Africa, and a portion of it flows into the southwest Indian Ocean, poleward of the Agulhas Current, where it joins the Indian Ocean's CDW layer (Mantyla & Reid, 1995; Talley, 2013). As the Indian Ocean is limited by continents northward of tropical latitudes, this CDW layer overturns in the northern Indian Ocean, entraining local intermediate waters to form Indian Deep Water (IDW). IDW flows back toward the SO, ultimately contributing to formation of both the Antarctic Intermediate Water (AAIW)/Subantarctic Mode Water (SAMW) and the CDW water masses (Talley, 2013). AAIW and SAMW lay above the CDW isopycnal (Figure 1b), while AAIW is primarily derived from SO waters, SAMW has inputs from subtropical surface water (SSW), indicated by its higher salinity. These warm and saline SSW are largely formed in the SIO basin (Beal et al., 2006), reflecting the excess evaporation over precipitation characteristic of subtropical gyre systems (Figure 1b).

DOC concentrations in the Indian Ocean are highest in the warm, subtropical surface waters (Doval & Hansell, 2000), with surface distributions variable and dependent on monsoon conditions (Hansell, 2009).
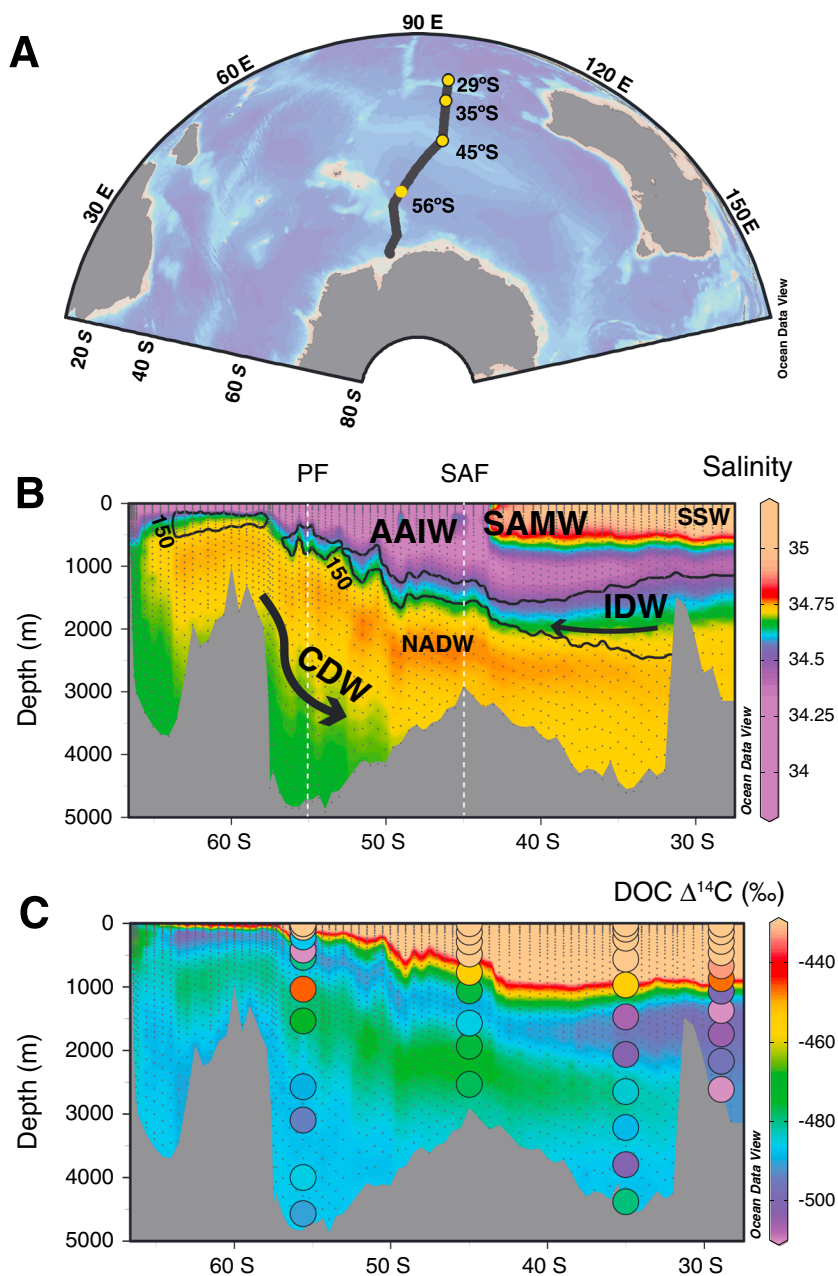
Figure 1. (a) Map depicting the 2016 occupation of GO-SHIP I08S. The I08S cruise track is outlined in black (stations occupied at 0.5° intervals); yellow symbols represent those stations where samples for DOC $\Delta^{14}C$ analyses were collected. (b) Section plot of salinity along I08S, with IDW contoured as waters containing AOU > 150 μmol kg^{-1}. Labeled deep water masses include the northward flowing CDW, the southward flowing IDW, and the intrusion of NADW originating from south of Africa (Talley, 2013), and AAIW, SAMW, and SSW. (c) Section plot of MLR-predicted DOC $\Delta^{14}C$ values (‰) with observed DOC $\Delta^{14}C$ values (‰) overlain in colored circles.

During monsoons, surface currents flush both the upper Bay of Bengal and Arabian Sea and ventilate the subtropical gyre waters. DOC that has accumulated at the surface in these regions is then redistributed and introduced into the subtropical gyre (Hansell, 2009). Unlike the surface DOC distributions, concentrations in the deep Indian Ocean are homogenously low, reflecting a mixture of their NADW and CDW source waters and showing no lasting signature of the exported surface-derived organic material (Doval & Hansell, 2000; Hansell, 2009; Hansell & Carlson, 1998; Hansell & Peltzer, 1998; Hansell et al., 2009). IDW plays a substantial role in CDW formation, accounting for ~35% of the total pool (Schmitz, 1995;

Talley, 2013). Consequently, DOC concentrations in CDW reflect a mixture of IDW, NADW, and Pacific Deep Waters (PDW) (Bercovici & Hansell, 2016). Our understanding of DOC dynamics in the Indian Ocean is incomplete; radiocarbon measurements of this pool of carbon can improve our knowledge.

2. Methods

2.1. Sampling for DOC Δ^{14}C

Samples were collected aboard the R/V *Revelle* in the austral summer of 2016 during the occupation of line I08S by the Global Ocean Ship-Based Hydrographic Investigation (GO-SHIP program; Figure 1a; data employed here are available in Tables S1–S4 in the supporting information; MacDonald et al,. 2016). Samples (~850 mL) were collected into 1 L precombusted amber glass bottles and immediately frozen at −20°C. Upper layer samples (those samples from depths <450 m) were filtered with 0.7 μM combusted GF/F filters to remove particulate organic material. Deep DOC Δ^{14}C samples were collected without filtration, as there is no resolvable difference in concentration between filtered and unfiltered DOC samples at depth (Hansell & Carlson, 2001). To ensure that there was no ^{14}C contamination aboard the R/V *Revelle*, SWAB tests (University of Miami) were conducted aboard the ship prior to departure. Swipe tests (Woods Hole Oceanographic Institute, WHOI) were conducted on the Niskin bottle spigots and air valves at two of the stations where DOC Δ^{14}C was sampled (stations 30 and 70). Both SWAB and swipe tests were within the acceptable ranges for natural abundance ^{14}C, indicating no measurable ^{14}C contamination on the ship or the CTD rosette where sampling occurred.

2.2. Radiocarbon Analyses

All DOC Δ^{14}C samples ($N = 45$) were processed at the National Ocean Science Accelerator Mass Spectrometer (NOSAMS) facility at WHOI. Thawed samples were acidified to pH 2 with phosphoric acid and purged with helium gas to remove inorganic carbon. Organic carbon was extracted from the water samples using UV oxidation and cryogenic extraction (following the method of Beaupré et al., 2007); sample sizes ranged from ~350 to ~700 μg C (supporting information Tables S1–S4). The resultant carbon (in the form of CO_2) was converted to graphite with H_2 on an iron catalyst and the ^{14}C atoms counted using the accelerator mass spectrometer (Longworth et al., 2015; McNichol et al., 1994; Roberts et al., 2010). At NOSAMS, instrumental precision was assessed using two types of DOC Δ^{14}C standards (oxalic acid and glycine), Milli-Q® blanks, and the standard error between repeated measurements of the same marine sample; this uncertainty in precision typically ranges from 2 to 10‰. The mean extraction efficiency (CO_2 recovered via cryogenic extraction divided by [DOC] ×100) of the radiocarbon data here is 99 ± 5%. Radiocarbon ages were derived from the DOC Δ^{14}C values following Stuiver and Polach (1977).

2.3. Hydrographic Measurements and DOC Concentrations

Salinity, temperature, and oxygen data were processed by the Scripps Oceanographic Data Facility and are publicly available at the GO-SHIP Carbon Hydrographic Data Office (CCHDO) website (https://cchdo.ucsd.edu/) (MacDonald et al., 2016). Apparent oxygen utilization (AOU) was calculated by subtracting measured oxygen from the saturation value computed at the potential temperature (θ) of the sample and 1 atm total pressure (Murray & Riley, 1969). Samples for [DOC] analysis were collected into glass vials and acidified with HCl on board; surface samples (depths <250 m) were filtered with precombusted 0.7 μM GF/F filters. [DOC] measurements were made in the laboratory (Carlson Laboratory, UC Santa Barbara) by high-temperature combustion (Carlson et al., 2010) and quality controlled using consensus reference material (deep-sea reference water, Hansell lab, University of Miami).

2.4. Analytical Approach Using Multiple Linear Regression

To assess the dynamic versus conservative properties of DOC Δ^{14}C, a Multiple Linear Regression (MLR) with salinity, θ, and AOU as our predictors was employed, following Bercovici and Hansell (2016). The MLR uses a singular value decomposition of the 45 DOC Δ^{14}C values and the predictors to estimate a conserved DOC Δ^{14}C value that would result solely from gradients between conserved parameters. The MLR equation is

$$\text{DOC } \Delta^{14}\text{C }_{MLR} = a_1 * \theta + a_2 * \text{sal} + a_3 * \text{AOU} + \beta \tag{1}$$

where θ is potential temperature in degrees, sal is the practical salinity, a_1-a_3 are the weights of each component, and β is the y intercept.

A

B

$$\Delta^{14}C_{MLR} = \Delta^{14}C_{obs}$$
$$R^2 = 0.96$$

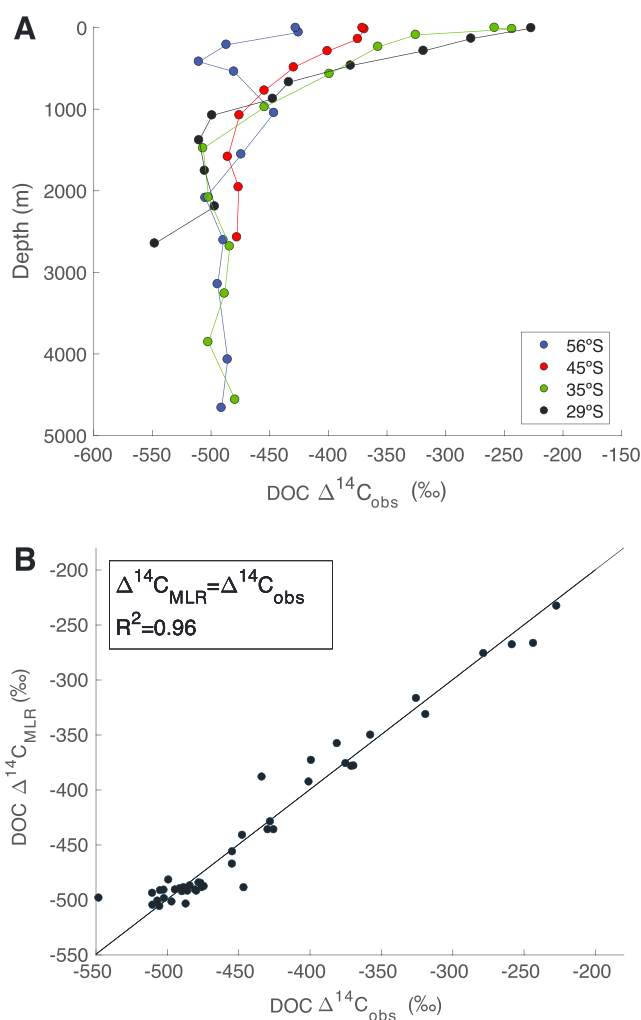**Figure 2.** (a) Depth profiles of DOC Δ^{14}C (‰) at the four different latitudes where we sampled. Errors for these data are ±6‰, based on standard measurements and duplicate analyses (sections 2.2 and 3). (b) Observed DOC Δ^{14}C values versus MLR-predicted DOC Δ^{14}C values of all samples (with a slope of 1, R^2 = 0.96, $p < 0.001$).

3. Results and Discussion

The radiocarbon profiles reported here sampled distinct water masses and latitude-dependent attributes, spanning from the Polar Front (PF) at 56°S to the subtropics at 29°S (Figures 1 and 2a). Data relevant to this analysis are provided in Tables S1–S4. The errors in the mean DOC Δ^{14}C values associated with water masses reported in the following subsections were propagated with the analytical uncertainty of the measurement (±6‰, median of the 2–10‰ analytical uncertainty (section 2.2)) following error propagation methods described by Taylor (1997).

3.1. DOC Δ^{14}C in SIO Surface Waters

The surface distribution of DOC Δ^{14}C reflects the difference in latitudes between the four occupied stations (Figure 2a). We isolated data from the surface layer as those above the mixed layer depth. Near the PF, (56°S; Figure 1a and Table S1), mean salinity was 33.79 ± 0.07, and θ ranged from 1.5 to 2.3°C (Figure 2b and Table S1). [DOC] were 42 μmol kg^{-1}, and DOC Δ^{14}C values had a mean of −426 ± 6‰ ($n = 2$, ~4,400 ^{14}C years; Table S1). Surface waters at the PF derive from aged, upwelled water masses; as such, [DOC] in surface waters in the SO are uniformly low (Hansell et al., 2009; Ogawa et al., 1999). This uniformity is observed in the radiocarbon data as well.

The Δ^{14}C values of the Antarctic surface waters reported here are more depleted than those reported at a similar latitude in the Pacific Sector of the SO (profile taken at 54°S, Druffel & Bauer, 2000); there, DOC Δ^{14}C values at depths <200 m had a mean of 390 ± 26‰ ($n = 5$, E. Druffel, personal communication, 2017). The Pacific samples were collected when average surface [DOC] were 50 ± 2 μmol kg^{-1} ($n = 6$, $d < 250$ m; Druffel & Bauer, 2000; E. Druffel, personal communication), whereas the average surface [DOC] reported here reached only 42 μmol kg^{-1} (Table S1).

Near the formation zone of SAMW at the Subantarctic Front (45°S; Figure 1a), there was more stratification in both the physical and biogeochemical variables of the system (Figure 1b and Table S2). Waters in the upper 1,000 m consisted of SAMW and AAIW. SAMW dominated the upper 400 m and had salinities of 34.0 to 34.5, θ of 9 to 10°C, [DOC] of 44 to 49 μmol kg^{-1}, and a mean DOC Δ^{14}C value of −379 ± 16‰

($n = 4$, ~3,800 ^{14}C years; Table S2). When including the SAMW that was present at 35°S and 28°S, the mean DOC Δ^{14}C value was less depleted at −366 ± 29‰ ($n = 9$), suggesting the incorporation of surface-derived DOC at these lower latitudes.

AAIW was immediately below SAMW (Table S2) and had salinities 34.3 to 34.4, θ from 4 to 7°C, and mean DOC Δ^{14}C values of −442 ± 19‰ ($n = 2$, ~4,600 ^{14}C years; Table S5). When incorporating the data from the lower latitude stations, the mean DOC Δ^{14}C value of AAIW was −444 ± 12‰ ($n = 5$). These similarities in the mean DOC Δ^{14}C values between AAIW at its formation and at lower latitudes imply that there is not a substantial amount of surface-derived DOC reaching the 500–1,000 m depths of AAIW.

In the subtropical SIO (35°S and 29°S), SSW were warm and stratified. In the upper 50 m, surface layer salinities reached 36.0 with [DOC] ranging from 60 to 70 μmol kg^{-1} (Figure 1b and Tables S3 and S4). Values for DOC Δ^{14}C in the SSW of the SIO subtropical gyre (upper 50 m) held a mean of −252 ± 22‰ ($n = 4$, ~2,000 to 2,300 ^{14}C years) and reflect the ^{14}C ages in subtropical gyres of other ocean regions. In the late 1980s, the subtropical North Atlantic and Central North Pacific (CNP) waters had SSW DOC Δ^{14}C values ranging from −210 to −280‰ (Druffel et al., 1992). In samples collected 20 years later, DOC Δ^{14}C values along 32°S ranged from −259‰ to −278‰ in the South Atlantic and −210‰ to −259‰ in the South Pacific (Druffel & Griffin,

2015; Druffel et al., 2016). Recently, in the surface waters north of Hawaii, DOC Δ^{14}C values ranged from $-180‰$ to $-250‰$ (Broek et al., 2017; Follett et al., 2014; Walker et al., 2011, 2016; Zigah et al., 2017); these results show that subtropical surface waters in all major ocean basins have similar ranges of DOC Δ^{14}C values.

3.2. DOC Δ^{14}C in Deep Water Masses of the SIO

While the surface radiocarbon ages changed with latitude, the hydrographic variables, DOC concentrations, and radiocarbon ages within the deep water masses showed greater homogeneity. Mean salinity in combined CDW/AABW at 56°S was 34.69 ± 0.03, while θ ranged from $-0.3°C$ in AABW to 2.2°C in CDW (Table S1). [DOC] were 39–40 μmol kg^{-1} and DOC Δ^{14}C values held a mean of $-468 ± 19‰$ ($n = 10$, Table S1 and Figures 1c and 2a). Here we refer to CDW and AABW as one water mass because there is no evidence that DOC from Antarctic shelves enriches [DOC] in AABW (Bercovici et al., 2017); without shelf inputs, [DOC] in AABW would be no different than that in CDW. There was one sample in CDW at 1047 m had a relatively less depleted DOC Δ^{14}C value of $-446‰$, which is taken to be an artifact of sampling and is an outlier with 95% confidence (Grubb's test, Grubbs, 1969). Excluding that value, the mean DOC Δ^{14}C value of the CDW pool at 55°S was $-491 ± 13‰$ ($n = 9$, ~5,400 ^{14}C years). These data are similar to those from the Pacific sector of the SO, where the mean DOC Δ^{14}C value was $-493 ± 23‰$ (~5,400 ^{14}C years; Druffel & Bauer, 2000; E. Druffel, personal communication). Reported DOC Δ^{14}C values in CDW here are relatively uniform throughout the water column; the same character is observed in previously reported deep data DOC Δ^{14}C values (Druffel & Bauer, 2000) indicating homogeneity in the massive pool of CDW surrounding Antarctica. CDW is present as well at 35°S, due to the depth of that station (Table S3). When combining the CDW from both 55°S and 35°S, the mean DOC Δ^{14}C value of CDW remains the same at 491 ± 13‰ ($n = 11$; Tables S1, S3, and S5).

At 45°S, CDW was largely absent because sampling was done above the relatively shallow (~3,000 m) Southeast Indian Ridge; NADW was the only deep water present at depths <3,000 m. At 45°S, NADW had θ of 2–3°C, [DOC] of 39 μmol kg^{-1} and a mean DOC Δ^{14}C value of $-479 ± 8‰$ ($n = 4$, ~5,200 ^{14}C years, Tables S2 and S5). NADW was also present at 35°S with similar mean [DOC] and AOU (Table S3); the mean DOC Δ^{14}C value of all NADW in the data set is $-481 ± 8‰$ ($n = 6$, ~5,200 years; Tables S2 and S5). NADW enters the southwest Indian Ocean at 5 Sverdrups (Talley, 2013), evident as a high-salinity core (Figure 1b) with relatively less depleted DOC Δ^{14}C values (Figure 1c). For comparison, NADW in the South Atlantic (defined in Druffel et al., 2016 as waters with depths >1,200 m) had mean DOC Δ^{14}C values of $-471 ± 8‰$ ($n = 19$; ~5,100 ^{14}C years, exact value from Druffel et al., 2016); the ages of NADW in the SIO are slightly older than those in the South Atlantic (Figures 1b and 1c and Tables S2 and S3), consistent with aging of the water mass as it transits into the Indian Ocean basin.

As IDW is the return flow of CDW upwelled and overturned in the northern Indian Ocean, it is characteristically an older water mass (Talley, 2013), with a high AOU due to oxygen minima originating from the north. As such, IDW was distinguishable in the SIO subtropical gyre stations between ~1,500 and 2,700 m, evidenced by its relatively high AOU (>150 μmol kg^{-1}; Figure 1b and Tables S3 and S4); [DOC] in IDW were 39 μmol kg^{-1}, and DOC Δ^{14}C values were the most depleted at $-511 ± 19‰$ ($n = 6$, ~5,700 ^{14}C years, Tables S3–S5). At 29°S, sampling was conducted over a ridge, so the water column reached only ~2,700 m; the deepest waters collected were solely IDW (Figure 1b and Table S4). The DOC Δ^{14}C value of the deepest sample at this station was the most depleted in the entire data set at $-548‰$ (~6,300 ^{14}C years, Table S4), anomalously older than the other ages of IDW and an outlier with >99% confidence (Grubbs, 1969). This anomalously depleted DOC Δ^{14}C value could be real; as the sample was collected on the Broken Ridge in the Southeast Indian Ocean, the depleted Δ^{14}C characteristic could be due to influence from a hydrothermal system (McCarthy et al., 2011). However, as there were unfortunately no duplicates, there is no way to confirm that this sample was not an artifact. The mean DOC Δ^{14}C value in IDW is $-503 ± 8‰$ ($n = 6$, ~5,600 ^{14}C years, Table S5) with the anomalous value removed. IDW has less depleted DOC Δ^{14}C values in comparison to PDW in the South Pacific ($-526‰$, ~5,900 ^{14}C years; Druffel & Griffin, 2015), likely due to its shorter residence time (Matsumoto, 2007; Stuiver et al., 1983) in the Indian Ocean basin as compared with PDW in the Pacific basin.

When comparing the DOC Δ^{14}C values between the different deep water masses, a two-tailed student's t test between CDW and IDW showed significant differences between the two data sets with >95% confidence

(p = 0.002, t = −2.58, degrees of freedom (d.f.) = 15); the same test between NADW and IDW additionally showed that those two water masses were significantly different with >99% confidence (p < 0.001, t = −7.5, d.f. = 10). However, there is no significant difference between CDW and NADW (student's t test, p = 0.08, t = −1.8). In any case, at 45°S, where there is the high salinity intrusion, indicative of NADW (Figure 1b; Mantyla & Reid, 1995), the DOC Δ^{14}C values are relatively low compared to surrounding deep waters (Figure 1c and Table S2).

3.3. MLR of Radiocarbon Data in the SIO

The coefficients for the MLR used to estimate a conserved DOC Δ^{14}C were as follows: a_1 = 5.5, a_2 = 36.6, a_3 = −0.5, and β = −1682 (equation (1) and section 2.4). The observed DOC Δ^{14}C values showed good agreement with the modeled DOC Δ^{14}C values in the MLR (Figure 2b, slope = 1, R^2 = 0.96, p < 0.001; d.f. = 43, residual mean standard error = 16‰), and the standard uncertainty of the MLR is 49‰ with 95% confidence (propagated using method from Farrance & Fernkel, 2012).

To assess the total uncertainty of the MLR, as well as the uncertainty associated with each water mass end-member, we used a Monte Carlo simulation (method described by Beaird et al., 2015). In the Monte Carlo simulation, each end-member tracer (i.e. salinity, θ, and AOU) was perturbed according to a random normal distribution with a mean equal to that of the chosen end-member value. The simulation solved the MLR for 500,000 perturbed realizations of end-member properties. The uncertainty of the MLR model was calculated as the standard error between the difference of the unperturbed and perturbed MLR solutions (Figure S1). The standard error of the Monte Carlo simulation of the entire MLR was 49‰, identical to that estimated with error propagation of the linear model.

The observed DOC Δ^{14}C values of each water mass in our analysis were not significantly different than those estimated by the MLR (student's t test; comparisons between mean observed and predicted DOC Δ^{14}C values for each water mass are in Table S5). These results suggest that the observed DOC Δ^{14}C values in the SIO track the gradients that are present in the conservative properties of water masses. In addition, due to the good agreement between the observed and MLR-predicted DOC Δ^{14}C values, the predicted DOC Δ^{14}C across the SIO basin can be visualized (Figure 1c). This good agreement is dependent on using data that sufficiently spans the gradients in the conserved parameters between latitudes and water masses (Figure 1b). When the data used in MLR is restricted by either of these parameters, the resultant coefficients do not accurately predict the larger-scale DOC Δ^{14}C distributions.

Another process that may cause anomalies in the MLR is the first-order decay of ^{14}C. As such, a linear approach can only be used where aging of waters is minimal. In this particular analysis, we use MLR because of the relatively small scale of the SIO basin; a parcel of deep water formed near Antarctica will resurface back at the Polar Front after 335 years in the Indian Ocean (Stuiver et al., 1983). Given the latitudinal span of the Indian Ocean (from Antarctica at 60°S to near 10°N near India), a parcel of water would take roughly 2 years to cross one latitudinal degree and thus 40 years to cross 20 latitudinal degrees. Further studies using CFC ages suggest that a parcel of AABW may move even faster into the SIO basin; these studies report a transit time into the Crozet basin (at ~32°S) to be between 15 and 25 years (Fine, 1993; Haine et al., 1998). These decadal transit times are within the error of the ^{14}C measurement (2 to 10‰ (section 2), ~30 to 90 ^{14}C years). In this analysis, there is a high correlation between the observed and modeled Δ^{14}C values, further suggesting that the aging effect is small.

4. Conclusions

We find that the gradients between the DOC Δ^{14}C values of IDW and CDW are consistent with respective placement in overturning circulation. In addition, the high-salinity NADW core holds less depleted DOC Δ^{14}C values, consistent with observations in the South Atlantic. Previous work estimated the residence times of deep waters relative to the Southern Ocean using Δ^{14}C values of dissolved inorganic carbon (Stuiver et al., 1983). That study reported residence times for the deep Indian and Pacific oceans to be 335 and 595 ^{14}C years, respectively. We see the same offsets relative to the Southern Ocean in DOC Δ^{14}C data; IDW is 5,600–5,700 ^{14}C years (Tables S1, S3, and S4), and PDW is 5,900–6,000 ^{14}C years (Druffel & Griffin, 2015), in comparison with the 5,300–5,400 ^{14}C year age of CDW. In addition, Druffel et al. (2016) showed that the age difference between the North and South Atlantic DOC Δ^{14}C samples was similar to the 225 ^{14}C year

replacement time as suggested by Stuiver et al. (1983). The similarity of the DOC $\Delta^{14}C$ offsets between different ocean basins with the replacement times suggested by Stuiver et al. (1983) implies that to a large extent, DOC is simply aging along the path of the ocean's deep conveyer.

However, even though the DOC $\Delta^{14}C$ values in the SIO largely reflect a conserved system, localized processes (local inputs) are likely occurring ephemerally. Recent studies suggest that the deep dissolved organic matter (DOM) pool is highly dynamic (Druffel & Griffin, 2015; Druffel et al., 2016; Follett et al., 2014), consisting of a complex mixture of compounds with various ages and reactivities (Broek et al., 2017; Flerus et al., 2012; Lechtenfeld et al., 2014; Loh et al., 2004; Walker et al., 2011, 2016; Zigah et al., 2017). While we are unable to assess the complexity of the DOM pool in the SIO, we find that the observed bulk DOC $\Delta^{14}C$ values are what is expected for in situ aging of DOC during deep ocean circulation; DOM dynamics do not override the ^{14}C signatures. These findings raise the question as to how DOC is both dynamic on a microscale and yet exhibits conservative behavior on a large scale.

References

Beaird, N., Straneo, F., & Jenkins, W. (2015). Spreading of Greenland meltwaters in the ocean revealed by noble gases. *Geophysical Research Letters*, *42*, 7705–7713. https://doi.org/10.1002/2015GL065003

Beal, L. M., Chereskin, T. K., Lenn, Y. D., & Elipot, S. (2006). The sources and mixing characteristics of the Agulhas Current. *Journal of Physical Oceanography*, *36*(11), 2060–2074. https://doi.org/10.1175/JPO2964.1

Beaupré, S. R., Druffel, E. R., & Griffin, S. (2007). A low-blank photochemical extraction system for concentration and isotopic analyses of marine dissolved organic carbon. *Limnology and Oceanography: Methods*, *5*(6), 174–184. https://doi.org/10.4319/lom.2007.5.174

Bercovici, S. K., & Hansell, D. A. (2016). Dissolved organic carbon in the deep Southern Ocean: Local versus distant controls. *Global Biogeochemical Cycles*, *30*, 350–360. https://doi.org/10.1002/2015GB005252

Bercovici, S. K., Huber, B. A., Dejong, H. B., Dunbar, R. B., & Hansell, D. A. (2017). Dissolved organic carbon in the Ross Sea: Deep enrichment and export. *Limnology and Oceanography*, *62*(6), 2593–2603. https://doi.org/10.1002/lno.10592

Broek, T. A. B., Walker, B. D., Guilderson, T. P., & McCarthy, M. D. (2017). Coupled ultrafiltration and solid phase extraction approach for the targeted study of semi-labile high molecular weight and refractory low molecular weight dissolved organic matter. *Marine Chemistry*, *194*, 146–157. https://doi.org/10.1016/j.marchem.2017.06.007

Carlson, C. A., Hansell, D. A., Nelson, N. B., Siegel, D. A., Smethie, W. M., Khatiwala, S., … Halewood, E. (2010). Dissolved organic carbon export and subsequent remineralization in the mesopelagic and bathypelagic realms of the North Atlantic basin. *Deep-Sea Research Part II*, *57*(16), 1433–1445. https://doi.org/10.1016/j.dsr2.2010.02.013

Doval, M., & Hansell, D. A. (2000). Organic carbon and apparent oxygen utilization in the western South Pacific and central Indian Oceans. *Marine Chemistry*, *68*(3), 249–264. https://doi.org/10.1016/S0304-4203(99)00081-X

Druffel, E. R. M., & Bauer, J. E. (2000). Radiocarbon distributions in Southern Ocean dissolved and particulate organic matter. *Geophysical Research Letters*, *27*, 1495–1498. https://doi.org/10.1029/1999GL002398

Druffel, E. R. M., & Griffin, S. (2015). Radiocarbon in dissolved organic carbon of the South Pacific Ocean. *Geophysical Research Letters*, *42*, 4096–4101. https://doi.org/10.1002/2015GL063764

Druffel, E. R. M., Griffin, S., Coppola, A. I., & Walker, B. D. (2016). Radiocarbon in dissolved organic carbon of the Atlantic Ocean. *Geophysical Research Letters*, *43*, 5279–5286. https://doi.org/10.1002/2016GL068746

Druffel, E. R. M., Williams, P. M., Bauer, J. E., & Ertel, J. R. (1992). Cycling of dissolved and particulate organic matter in the open ocean. *Journal of Geophysical Research: Oceans*, *97*, 15,639–15,659. https://doi.org/10.1029/92JC01511

Farrance, I., & Frenkel, R. (2012). Uncertainty of measurement: A review of the rules for calculating uncertainty components through functional relationships. *The Clinical Biochemist Reviews*, *33*(2), 49–75.

Fine, R. A. (1993). Circulation of Antarctic intermediate water in the south Indian ocean. *Deep-Sea Research Part I*, *40*(10), 2021–2042. https://doi.org/10.1016/0967-0637(93)90043-3

Flerus, R., Lechtenfeld, O. J., Koch, B. P., McCallister, S. L., Schmitt-Kopplin, P., Benner, R., … Kattner, G. (2012). A molecular perspective on the ageing of marine dissolved organic matter. *Biogeosciences*, *9*, 935–1955.

Follett, C. L., Repeta, D. J., Rothman, D. H., Xu, L., & Santinelli, C. (2014). Hidden cycle of dissolved organic carbon in the deep ocean. *Proceedings of the National Academy of Sciences of the United States of America*, *111*(47), 16,706–16,711. https://doi.org/10.1073/pnas.1407445111

Gordon, A. L. (1985). Indian-Atlantic transfer of thermocline water at Agulhas retroflection. *Science*, *227*(4690), 1030–1033. https://doi.org/10.1126/science.227.4690.1030

Grubbs, F. E. (1969). Procedures for detecting outlying observations in samples. *Technometrics*, *11*(1), 1–21. https://doi.org/10.1080/00401706.1969.10490657

Haine, T. W. N., Watson, A. J., Liddicoat, M. I., & Dickson, R. R. (1998). The flow of Antarctic bottom water to the southwest Indian Ocean estimated using CFCs. *Journal of Geophysical Research*, *103*, 27,637–27,653. https://doi.org/10.1029/98JC02476

Hansell, D. A. (2009). Dissolved organic carbon in the carbon cycle of the Indian Ocean. In J. D. Wiggert, et al. (Eds.), *Indian Ocean biogeochemical processes and ecological variability* (Vol. 185, pp. 217–230). Washington, DC: American Geophysical Union. https://doi.org/10.1029/2007GM000684

Hansell, D. A., & Carlson, C. A. (1998). Deep ocean gradients in dissolved organic carbon concentrations. *Nature*, *395*(6699), 263–266. https://doi.org/10.1038/26200

Hansell, D. A., & Carlson, C. A. (2001). Biogeochemistry of total organic carbon and nitrogen in the Sargasso Sea: Control by convective overturn. *Deep-Sea Research Part II*, *48*(8-9), 1649–1667. https://doi.org/10.1016/S0967-0645(00)00153-3

Hansell, D. A., Carlson, C. A., Repeta, D. J., & Schlitzer, R. (2009). Dissolved organic matter in the ocean: New insights stimulated by a controversy. *Oceanography*, *22*, 52–61.

Hansell, D. A., & Peltzer, E. T. (1998). Spatial and temporal variations of total organic carbon in the Arabian Sea. *Deep-Sea Research Part II*, *45*(10-11), 2171–2193. https://doi.org/10.1016/S0967-0645(98)00067-8

Lechtenfeld, O. J., Kattner, G., Flerus, R., McCallister, S. L., Schmitt-Kopplin, P., & Koch, B. P. (2014). Molecular transformation and degradation of refractory dissolved organic matter in the Atlantic and Southern Ocean. *Geochimica et Cosmochimica Acta*, *126*, 321–337. https://doi.org/10.1016/j.gca.2013.11.009

Loh, A. N., Bauer, J. E., & Druffel, E. R. M. (2004). Variable aging and storage of dissolved organic components in the open ocean. *Nature*, *430*(7002), 877–881. https://doi.org/10.1038/nature02780

Longworth, B. E., von Reden, K. F., Long, P., & Roberts, M. L. (2015). A high output, large acceptance injector for the NOSAMS Tandetron AMS system. *Nuclear Instruments and Methods in Physics Research B*, *361*, 211–216. https://doi.org/10.1016/j.nimb.2015.04.005

MacDonald, A., et al. (2016). GO-SHIP I08S, data file: '33RR20160208_hy1.csv'. [Retrieved from https://cchdo.ucsd.edu/cruise/33RR20160208.], CLIVAR and Carbon Hydrographic Data Office, La Jolla, CA, USA, 02/2016, doi:10.7942/C2H59N.

Mantyla, A. W., & Reid, J. L. (1995). On the origins of deep and bottom waters of the Indian Ocean. *Journal of Geophysical Research*, *100*, 2417–2439. https://doi.org/10.1029/94JC02564

Matsumoto, K. (2007). Radiocarbon-based circulation age of the world oceans. *Journal of Geophysical Research*, *112*, C09004. https://doi.org/10.1029/2007JC004095

McCarthy, M. D., Beaupré, S. R., Walker, B. D., Voparil, I., Guilderson, T. P., & Druffel, E. R. M. (2011). Chemosynthetic origin of ^{14}C-depleted dissolved organic matter in a ridge-flank hydrothermal system. *Nature Geoscience*, *4*(1), 32–36. https://doi.org/10.1038/ngeo1015

McNichol, A. P., Osborne, E. A., & Gagnon, A. R. (1994). TIC, TOC, DIC, DOC, PIC, POC - unique aspects in the preparation of oceanographic samples for C-14 AMS. *Nuclear Instruments and Methods in Physics Research B*, *92*(1-4), 162–165. https://doi.org/10.1016/0168-583X(94)95998-6

Murray, C. N., & Riley, J. P. (1969). The solubility of gases in distilled water and seawater. 2. Oxygen. *Deep-Sea Research*, *16*, 311–320.

Ogawa, H., Fukuda, R., & Koike, I. (1999). Vertical distributions of dissolved organic carbon and nitrogen in the Southern Ocean. *Deep-Sea Research Part I*, *46*(10), 1809–1826. https://doi.org/10.1016/S0967-0637(99)00027-8

Roberts, M. L., Burton, J. R., Elder, K. L., Longworth, B. E., McIntyre, C. P., von Reden, K. F., … McNichol, A. P. (2010). A high-performance ^{14}C Accelerator Mass Spectrometry system. *Radiocarbon*, *52*(02), 228–235. https://doi.org/10.1017/S0033822200045252

Schmitz, W. J. (1995). On the interbasin-scale thermohaline circulation. *Reviews of Geophysics*, *33*, 151–173. https://doi.org/10.1029/95RG00879

Stuiver, M., & Polach, H. (1977). Discussion of reporting of ^{14}C data. *Radiocarbon*, *19*(3), 355–363.

Stuiver, M., Quay, P., & Oslund, H. G. (1983). Abyssal water carbon-14 distribution and the age of the world oceans. *Science*, *219*(4586), 849–851. https://doi.org/10.1126/science.219.4586.849

Talley, L. D. (2013). Closure of the global overturning circulation through the Indian, Pacific, and Southern Oceans: Schematics and transports. *Oceanography*, *26*(1), 80–97. https://doi.org/10.5670/oceanog.2013.07

Taylor, J. R. (1997). *An introduction to error analysis: The study of uncertainties in physical measurements* (2nd ed.). Saussalito, CA: University Science Books.

Walker, B., Beaupré, S., Guilderson, T., Druffel, E., & McCarthy, M. (2011). Large-volume ultrafiltration for the study of radiocarbon signatures and size vs. age relationships in marine dissolved organic matter. *Geochimica et Cosmochimica Acta*, *75*(18), 5187–5202. https://doi.org/10.1016/j.gca.2011.06.015

Walker, B. D., Beaupre, S., Guilderson, T. P., McCarthy, M. D., & Druffel, E. R. M. (2016). Pacific carbon cycling constrained by organic matter size, age and composition relationships. *Nature Geoscience*, *9*(12), 888–891. https://doi.org/10.1038/ngeo2830

Zigah, P. K., McNichol, A. P., Xu, L., Johnson, C., Santinelli, C., Karl, D. M., & Repeta, D. J. (2017). Allochthonous sources and dynamic cycling of ocean dissolved organic carbon revealed by carbon isotopes. *Geophysical Research Letters*, *44*, 2407–2415. https://doi.org/10.1002/2016GL071348